sLHC Project Note 0013

2010-02-04

Christoph.Hessler@cern.ch

PS2 Transfer Lines

C. Hessler, B. Goddard, M. Meddahi / TE-ABT

Keywords: PS2, transfer lines, H^- beam line, optics, trajectory correction, injection, extraction

Summary

Within the scope of the LHC injector upgrade it has been proposed to replace the present injector chain by new accelerators, LINAC4, SPL and PS2, for which new transfer lines will be required. In this report the beam line properties and requirements are summarized. Then the initial optics of these beam lines and their geometry are discussed. Particular attention is given to the injection and extraction regions where several beam lines have to intersect, imposing challenging constraints on the layout. Directions for optimisation are suggested.

1. Introduction

In order to maximize the physics reach of the LHC there is a strong motivation to increase the integrated luminosity. This can be achieved by increasing the peak luminosity and/or the beam availability. Apart from upgrading the LHC itself, higher peak luminosity can also be achieved by beams of higher intensity and better quality than possible with the current injectors. Furthermore, availability and reliability of the injector chain is limited by the age of the accelerators which have been constructed between 1959 and 1978.

To overcome these limitations, an upgrade of the present injector chain has been proposed by the study group on Proton Accelerators for the Future (PAF) [1]. Within this upgrade plan it is proposed to replace the existing 50 MeV proton linear accelerator LINAC2, the PS Booster synchrotron and the 26 GeV proton synchrotron (PS) by new machines and to implement extensive system upgrades in the SPS.

The presently proposed new LHC injector chain consists of a 160 MeV linear accelerator (LINAC4 [2]), a superconducting H^- linac (SPL [3]) and a new 50 GeV proton synchrotron (PS2 [4]). These machine designs are flexible, to leave open the possibility to use them as drivers for future experimental facilities like a new fixed target area or a new neutrino facility. Hence, there exists a low power (LP-SPL) and a high power (HP-SPL) design version of the SPL delivering beams with kinetic energies of 4 and 5 GeV and beam powers of 0.2 and 4 MW, respectively. An interesting additional option might be to operate the SPL at 5 GeV but with low power beams (LP-SPL-5G).

The main beam parameters of the different SPL versions and the PS2 are listed in Tab. 1 and Tab. 2, respectively. The foreseen location of the SPL is in the prolonged LINAC4 tunnel parallel to the TT10 transfer line from PS to SPS. PS2 is planned to be installed between SPL and SPS in the plane of the SPS (Fig. 1).

Table 1: SPL beam parameters.

Parameter	**LP-SPL**	**LP-SPL-5G**	**HP-SPL**
Kin. energy [GeV]	4	5	5
Beam power [MW]	0.192	0.24	4
Repetition rate [Hz]	2	2	50
Particles per pulse	$1.5 \cdot 10^{14}$	$1.5 \cdot 10^{14}$	$1.0 \cdot 10^{14}$
Pulse length [ms]	1.2	1.2	0.4
Average/peak pulse current [mA]	20/32	20/32	40/64
Max. fract. loss [m^{-1}]	$5.2 \cdot 10^{-7}$	$4.17 \cdot 10^{-7}$	$2.5 \cdot 10^{-8}$
Max. B field [T] (see section 3.1)	0.115	0.0950	0.0858
Min. bend. radius [m]	141	206	228
Norm. emittance H/V [µm]	0.35/0.35	0.35/0.35	0.35/0.35

Table 2: PS2 beam parameters. In this paper, all ion beam energies are given as proton equivalent energies based on the relation between the ion momentum per nucleon p_N and the proton equivalent momentum $p_p = p_N \cdot A/Z$. For example, a proton equivalent energy of 50 GeV of a $^{208}Pb^{54+}$ beam corresponds to 12.3 GeV/nucleon.

Parameter	**PS2 (protons)**	**PS2 (ions)**
Geometry	Racetrack	
Circumference [m]	1346.4	
Kin. injection energy [GeV]	4	1.3
Kin. extraction energy [GeV]	20-50	20-50
Norm. emittance H/V for LHC operation [µm]	3/3	1/1
Norm. emittance H/V for CNGS operation [µm]	9/6	-

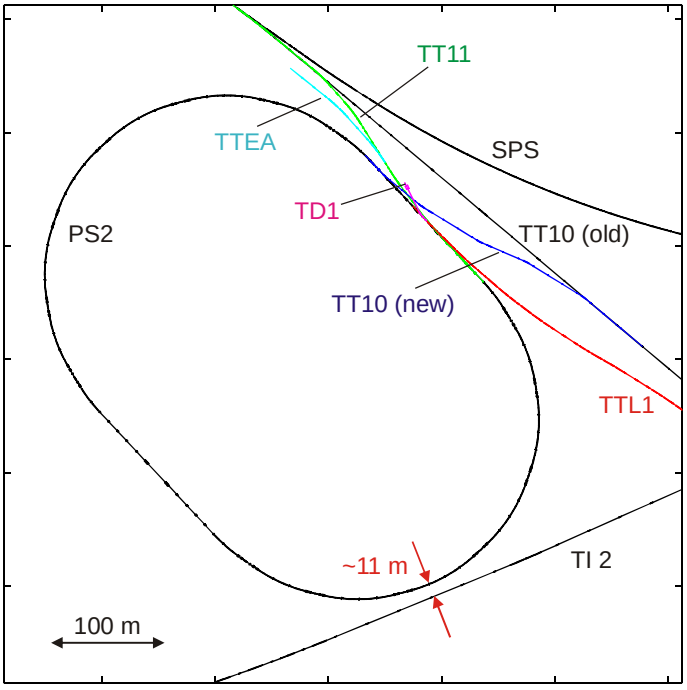

Figure 1 Schematic overview of the PS2 and its injection and extraction transfer lines

2. Injection and extraction systems

For the new injector chain a number of beam transfer systems for injection, extraction, beam dumping and beam transfer are required.

PS2 injection:

- Fast single-turn injection of ions at 1.3 GeV and protons of 1.3 GeV for PS2 commissioning;
- Multi-turn H^- injection at 4 GeV with stripping foil and laser stripping.

PS2 extraction:

- Fast single-turn extraction of protons and ions at 20-50 GeV for SPS;
- Slow extraction of protons for the PS2 experimental area.

PS2 beam dumps:

- Injection beam dump for unstripped and partially stripped H^-/H^0 waste beams.
- External beam dump for all kind of beams

Transfer lines and their preliminary names:

- PS/LEIR to PS2 (TT10), 1.3 GeV ions/protons;
- SPL to PS2 (TTL1), 4/5 GeV H^-;
- PS2 to SPS (TT11), 20-50 GeV protons/ions;
- PS2 to PS2 experimental area and external beam dump (TTEA), 20-50 GeV protons/ions;
- PS2 to H^- beam dump (TD1), 4/5 GeV protons.

The basic properties of the various PS2 transfer lines are summarized in Tab. 3. In order to have enough space to equip in particular the beam line to the SPS (TT11) with all necessary systems, which will be discussed later, the extraction point is located upstream of the injection points in the PS2 Long Straight Section 1 (LSS1, Fig. 2, [5]). As a result the injection and extraction beam lines are longer, as desired, but cross each other at several points (Fig. 1). The detailed geometry of these intersections will be discussed later. The studies presented in the following chapters are all based on the PS2 lattice version from 17th Dec 2008 and on the SPL lattice version from end of 2008. In this version, the long PS2 injection/extraction straight section is based on 90 degree FODO cells with a central symmetric doublet for the H^- stripping insertion.

Table 3: Beam line properties.

Beam line	Energy	Particle type	Length	Version	Features
TT11, slow/fast extraction	20 – 50 GeV	Protons, Pb^{54+}/Pb^{82+} ions	~ 375 m	7.2.3.2	Emittance exchange, low beta section for ion stripping
TT10, fast injection	1.3 – 4 GeV	Protons, Pb^{54+} ions from LEIR	~ 300 m from QID1015	0.2.3	For commissioning and ion operation
TTL1, multi-turn injection	4 – 5 GeV	H^-	~ 410 m	0.2.10	Max. dipole field limited by Lorentz stripping
TD1	4 GeV	Protons	~ 40 m	0.0.3	To beam dump
TTEA	20 – 50 GeV	Protons, Pb^{54+} ions	TBD	0.0.1	To (underground) experimental area / external beam dump

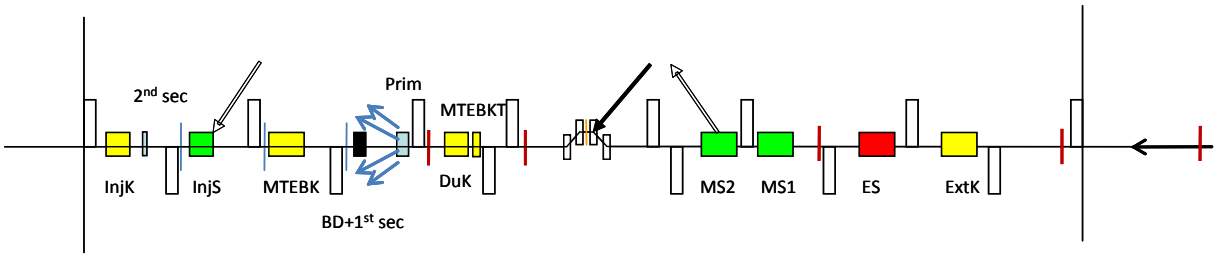

Figure 2 Long straight section 1 (LSS1) of the PS2 with the injection and extraction elements (Courtesy W. Bartmann)

3. TTL1 transfer line

This beam line will link the SPL to the PS2. The low power H^- beam will be injected into the PS2 by charge-exchange injection over a few hundred turns. In addition to the classical use of a foil to strip the electrons off the H^- ions, a laser stripping scheme is also under study [6]. The first part of TTL1 will potentially be used for the transport of HP-SPL beams up to the point where a beam line to a future neutrino facility can branch off and must therefore be compatible with all SPL beam types. However, the second part needs to be compatible only with the 4 and optionally with the 5 GeV versions of the LP-SPL.

3.1 Beam loss limitations

One important feature of H^- beams is that the loosely-bound outer-shell electron can be easily removed in strong magnetic fields, due to the so-called Lorentz-stripping. To limit the resulting beam loss and to prevent radiation protection issues, the magnetic fields of the beam line elements must not exceed a certain threshold. The maximum B field can be calculated from the maximum fractional loss rate *df/ds* using the following equation (from [7]):

$$\frac{df}{ds} = \frac{B}{A_1}\exp\left(-\frac{A_2}{\beta_r \gamma_r cB}\right) \qquad (1)$$

With β_r and γ_r being the relativistic β and γ factors, c is the light velocity and A_1=2.47•10^{-6} Vs/m and A_2=4.49•10^9 V/m are constants [7]. The maximum acceptable fractional loss can be obtained from the maximum power loss which should be less than 0.1 W/m for TTL1. Figure 3 shows the simulated power loss for the different SPL beam types as a function of the magnetic field. The resulting curves are rather steep. Therefore, even a small decrease of the magnetic field can reduce the power loss drastically. The calculated limits for the magnetic fields and the corresponding bending radii are listed in Tab. 1.

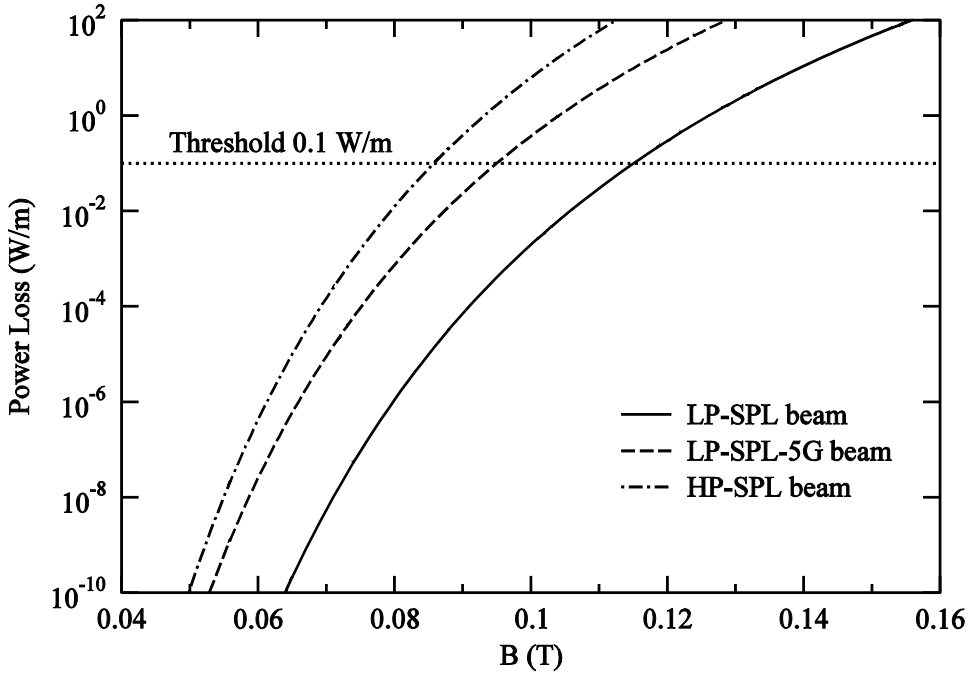

Figure 3 Power loss as a function of the magnetic field for 4 and 5 GeV LP-SPL and 5 GeV HP-SPL beams. The power loss in TTL1 should be less than 0.1 W/m

3.2 Geometrical constraints

The start and end points of the TTL1 transfer line are the SPL end point and the stripping foil location in the PS2, respectively. Their coordinates in the CERN Coordinate System (CCS) [8] are listed in Tab. 4. Between these points TTL1 has to cross existing tunnels e.g. of the TI 2 transfer line. To ensure a sufficient distance between TTL1 and TI 2 an additional fixed point C has been added to the TTL1 geometry constraints [9] (Tab. 4, Fig. 4).

Over a total distance of only 410 m the beam line has to overcome an altitude difference of 21 m. However, due to the point C constraint, the beam line must maintain, up to this point, only the moderate -1.5 % slope of the SPL tunnel. Furthermore, as a result of the bending field limitation, the beam line can be bent only smoothly, so that the maximum slope of the remaining part of the tunnel yields a large value of -8.1 %.

Table 4: CCS coordinates of important points of TTL1 (in beam direction).

Point	X [m]	Y [m]	Z [m]	Bearing [rad]	Slope [rad]
Starting point	1510.09247	2278.25946	2423.58630	-0.87159	-0.015085
Point C	1470.71439	2311.37371	2422.81006	-0.87159	-0.015085
Stripping foil	1187.20290	2521.95506	2402.14771	-0.75042	-0.000207

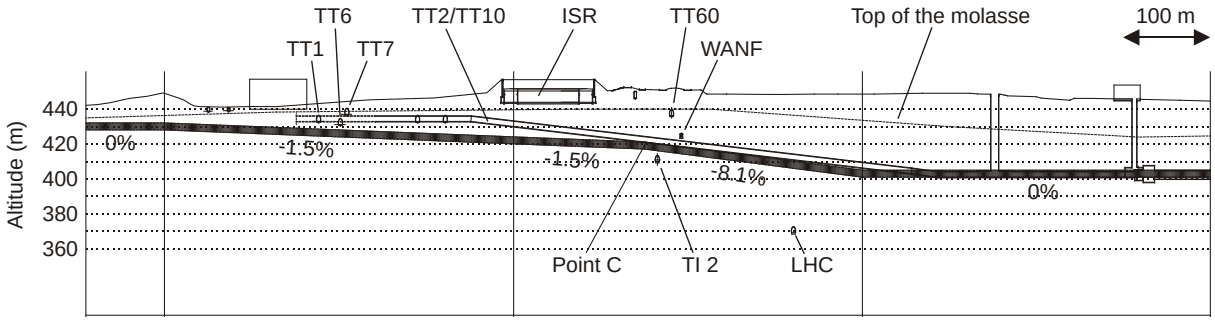

Figure 4 Sketch of the longitudinal tunnel section of TTL1 showing the various crossing tunnels. The beam line must be bent more smoothly than indicated between point C and the PS2 due to the Lorentz stripping limit

3.3 Beam line layout

Based on these constraints, the beam line layout shown in Fig. 5 has been proposed for TTL1. It consists of a regular FODO lattice with 90 degrees phase advance per cell and a cell length of 25 m which is matched to the SPL and PS2 using 4 and 9 quadrupole magnets, respectively. The Twiss parameters at these matching points are listed in Tab. 5. The bending of the H^- beam is performed with 2 combined horizontal and vertical achromats at the start (after point C) and at the end of the line and 2 horizontal achromats in between. In the achromats the dipole magnets have been arranged in equally powered pairs with 180 degrees phase advance to cancel their dispersion effects.

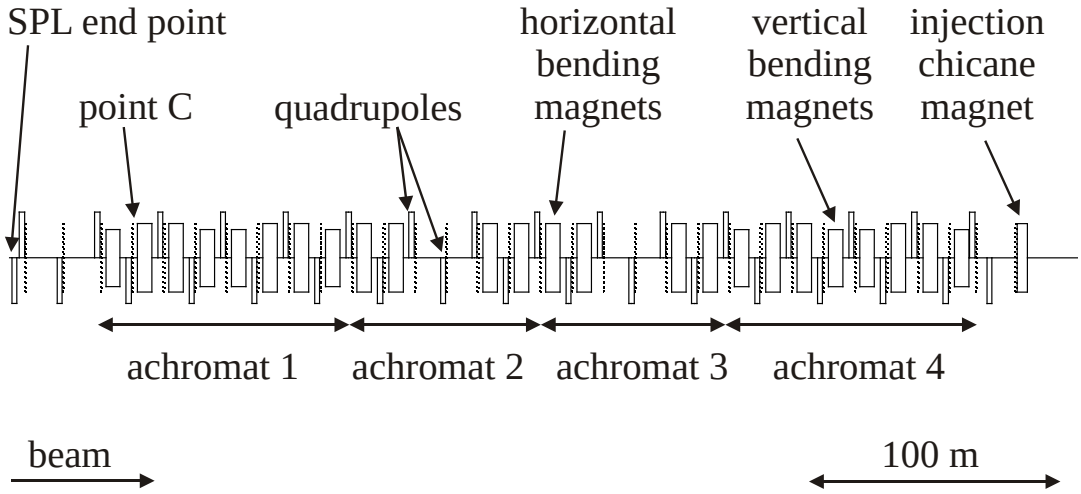

Figure 5 Beam line layout of the TTL1 transfer line

Table 5: Twiss parameters at the start and at the end of the TTL1 beam line (in beam direction).

Point	**Plane**	**β [m]**	**α**	**D [m]**	**D'**
SPL end point	X	106.5	-0.055	0	0
	Y	117.3	-1.352	0	0
Stripping foil	X	15	0	-0.4	0
	Y	15	0	0	0

In the present design, these achromats consist of 5.75 m long dipole magnets which could possibly be made from former LEP dipole magnet yokes, equipped with new coils. These magnets would be ideally suited for the TTL1 transfer line due to their low magnetic field. With this magnet type the beam loss requirements are fulfilled for HP-SPL beams in the first two achromats and for 4 GeV LP-SPL beams in all four achromats (Tab. 6). Therefore, the first half of the beam line could indeed be used as transfer line to a future neutrino facility, which could branch off TTL1 at the empty cell in the middle of the second achromat. However, with this configuration, the transfer of 5 GeV LP-SPL beams is not possible towards PS2. If this feature is needed 7.2 m long dipole magnets could be used instead.

Table 6: TTL1 dipole magnet parameters.

Dipole Family	Achromat	Quantity	Angle [rad]	B [T] @ 4 GeV	B [T] @ 5 GeV
Vertical 1	1	4	0.0164	0.0462	0.0559
Horizontal 1	1, 2	8	-0.0238	0.0668	0.0807
Horizontal 2	3, 4	8	0.0339	0.0953	0.1153
Vertical 2	4	4	-0.0200	0.0563	0.0681

3.4 Optics simulations

For the layout described above, detailed optics simulations at zero beam current have been carried out using MAD-X [10]. The resulting beta and dispersion functions are plotted in Fig. 6. The quadrupoles of the last achromat were detuned in order to obtain the required dispersion value of -0.4 m in the horizontal plane at the stripping foil of the PS2.

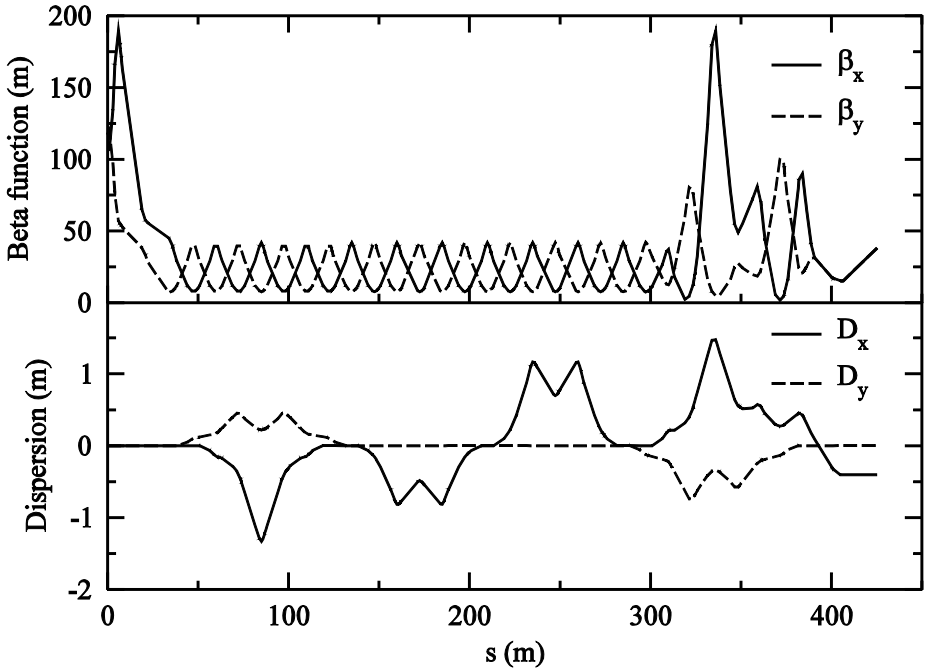

Figure 6 Simulated beta and dispersion functions along the TTL1 transfer line for a 4 GeV H^- beam using MAD-X

3.5 Aperture calculation

In addition to optics simulations, aperture calculations of the TTL1 transfer line have been carried out with MAD-X. The resulting beam envelopes shown in Fig. 7 were calculated using the following equation:

$$x, y = N \cdot \sigma \cdot 1.1 + |D| \cdot \frac{\Delta p}{p} \cdot 1.1 + co \cdot \sqrt{\frac{\beta}{\beta_{\max}}} \qquad (2)$$

In this equation, σ is the r.m.s. beam size, D and β are the dispersion and beta functions, $\Delta p/p$ is the momentum spread and co is the maximum allowed trajectory excursion. For the calculations, a $6\,\sigma$ beam size, the SPL normalized emittances of 0.35 μm and a 5 mm trajectory excursion have been used. From the energy spread ΔE_{rms}=0.887 MeV of the 5 GeV HP-SPL beam, the momentum spread $\Delta p/p = 1.53 \cdot 10^{-4}$ has been calculated and assumed to be the same for 4 GeV beams.

Figure 7 shows that for the calculated beam envelopes a half aperture of 30 mm would be sufficient in the whole TTL1 beam line. In the regular cells a half aperture of 15 mm would even be possible in both planes, since the SPL emittance is so small. The aperture requirements of the magnets are summarized together with the further specifications in Tab. 7.

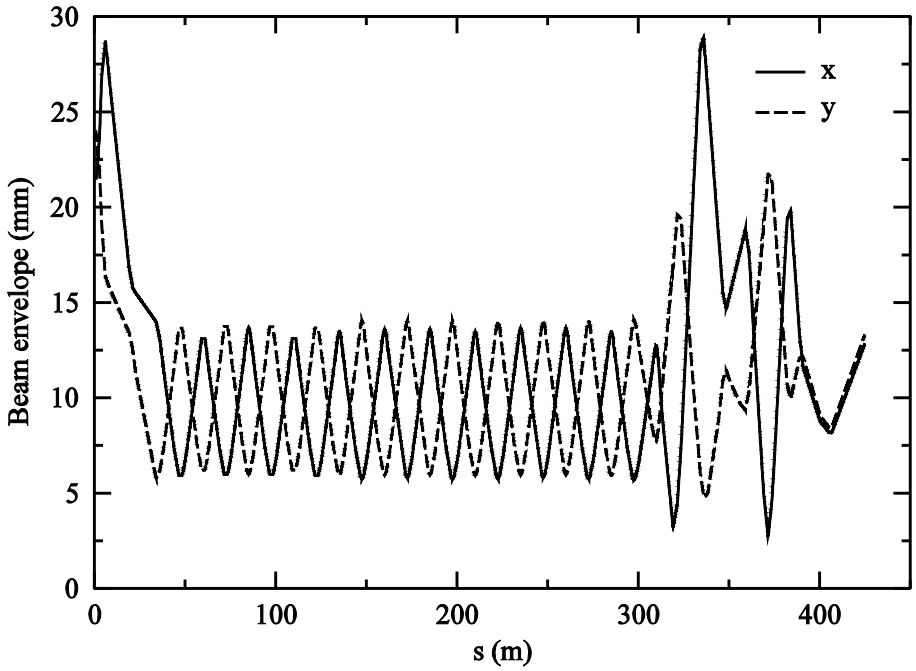

Figure 7 Plot of the calculated beam envelopes of TTL1 in the horizontal and vertical plane for a 4 GeV beam

Table 7: Draft TTL1 magnet specifications.

Magnet type	**Max. gradient or max. field**	**Length**	**Max. K or max. α**	**Number**	**Half aperture H/V**
MQ main	2 T/m	2.0 m	0.11 m^{-2}	33	0.03 m / 0.03 m
MBH	0.12 T	5.75 m	0.04 rad	16	0.03 m / 0.03 m
MBV	0.12 T	5.75 m	0.04 rad	8	0.03 m / 0.03 m

3.6 Trajectory correction

For TTL1 three different trajectory correction schemes have been studied with MAD-X:

- Every quadrupole equipped with one dual plane beam position monitor (BPM) and one horizontal or vertical corrector (referred to as 1-in-1 scheme);
- Every third corrector and monitor has been dropped from the 1-in-1 scheme (2-in-3 scheme);
- Each quadrupole equipped with one monitor, two consecutive quadrupoles out of three equipped with correctors (combined 1-in-1 / 2-in-3 scheme).

For all schemes the errors listed in Tab. 8 have been assumed. The combined scheme was identified to be the optimum solution in view of the costs and the stability: Whereas the stability is comparable to the 1-in-1 scheme, the costs are lower. The 2-in-3 scheme, however, produces larger trajectory excursions, especially in the case of monitor failures. Furthermore, it is essential for all schemes that BPMs are equipped with dual plane measurements.

Figure 8 shows a plot of 100 simulated uncorrected and corrected trajectories for the combined scheme. The used corrector strength is below 0.04 T and the trajectory excursions are in most cases less than 1 mm, which is within the specification. However, there exist a few rare cases where the correction system fails. This might happen if one of the two last monitors or two consecutive monitors fail.

Table 8: Assumed errors in the TTL1 beam line.

Error	**Distribution / value**
Quadrupole displacement in x/y plane	Gaussian, σ = 0.2 mm, cut at 3 σ
Dipole field	Gaussian distribution of deflection angle with σ = 10 µrad (corresponds to a relative field error of $5 \cdot 10^{-4}$), cut at 2 σ
Dipole tilt	Gaussian, σ = 0.2 mrad, cut at 4 σ
Monitor read errors in x/y plane	Flat random distribution of ±0.5 mm
Injection error	Gaussian distribution of position and angle with σ = 0.5 mm and 0.05 mrad, cut at 2 σ
Monitor failure probability	5 %

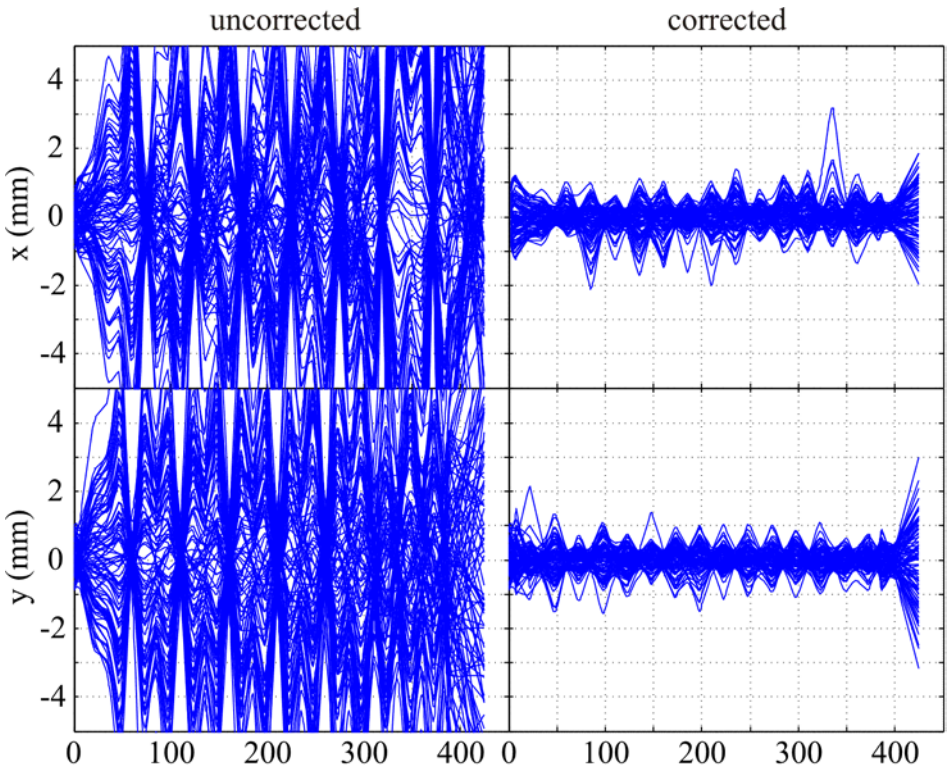

Figure 8 Plot of 100 uncorrected and corrected trajectories for the chosen combined 1-in-1 / 2-in-3 scheme

4. TT10 transfer line

The TT10 beam line currently links the PS and SPS and will have to be redesigned to link the PS to the future PS2. A new tunnel will be required between the present TT10 transfer line and the PS2. The main purpose of the future TT10 line will be to transport heavy ion beams from LEIR to the PS2 with a magnetic rigidity equivalent to 1.3 GeV protons and to provide 1.3 GeV proton beams for the PS2 commissioning phase. The beams will be injected into PS2 by fast injection.

4.1 Beam line geometry

The new part of TT10 starts at the end of the quadrupole QID1015 of the present TT10 transfer line and arrives in the PS2 a few meters in front of the LSS1 end point. For convenience, the LSS1 end point was taken as end point of TT10 for the simulations. The CCS survey coordinates of these points are listed in Tab. 9. One horizontal and one combined horizontal/vertical achromat are used to transport the beam from the existing TT10 beam line to the PS2 plane. The layout of the beam line is shown in Fig. 9.

Table 9: CCS coordinates of important points of TT10 (in beam direction).

Point	X [m]	Y [m]	Z [m]	Bearing [rad]	Slope [rad]
QID1015 end	1377.47447	2411.26847	2413.22528	-0.87159	-0.059571
LSS1 end point	1137.18775	2575.39180	2402.13258	-0.75042	-0.000207

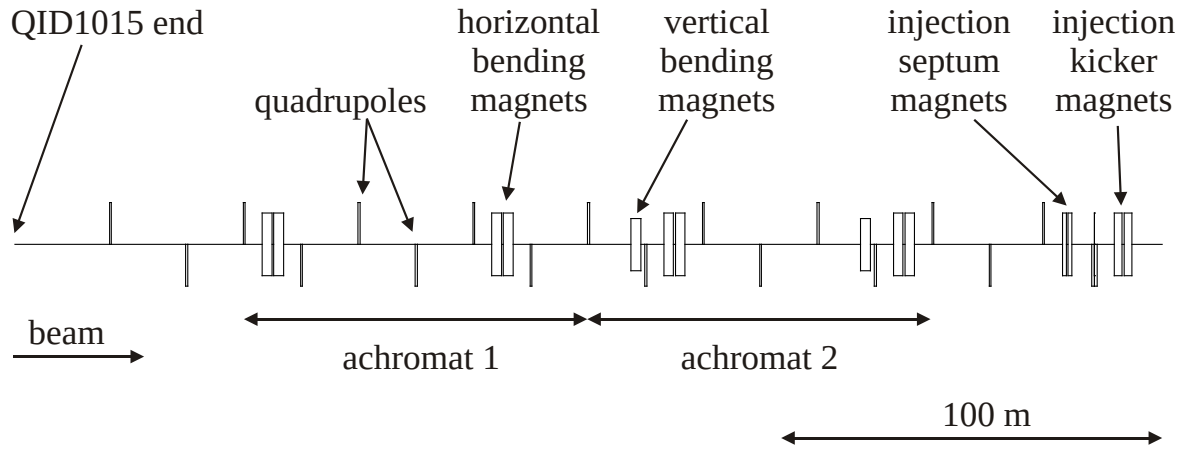

Figure 9 Beam line layout of the new part of the TT10 transfer line which starts at the quadrupole QID1015 of the present TT10 beam line

Since the existing TT10 transfer line has a FODO lattice with approximately 90 degrees phase advance per cell, the same choice has also been made for the new part of the line. To adapt the cell length of 60.496 m in TT10 to the FODO cell length of 23.21 m in the LSS1 of PS2 an intermediate cell length of 30 m has been chosen for the new part. This ensures as well the availability of enough degrees of freedom for matching TT10 to PS2 by a sufficient number of individually powered quadrupoles in the new part of the line. The new part is fully matched to the existing part of TT10 and to the PS2. The corresponding Twiss parameters at the matching points are shown in Tab. 10.

Table 10: Twiss parameters at the start and the end of the new part of the TT10 transfer line (in beam direction).

Point	**Plane**	**β [m]**	**α**	**D [m]**	**D'**
QID1015 end	X	19.219	-0.490	1.609	0.125
	Y	114.475	2.924	5.419	-0.125
LSS1 end point	X	33.923	-2.073	0	0
	Y	12.494	0.810	0	0

4.2 Optics simulations

Detailed optics simulations have been carried out for this beam line design using MAD-X. The simulated beta and dispersion functions are shown in Fig. 10. Using the dispersion suppressor scheme the large dispersion oscillations in the present TT10 line can be reduced to zero at the LSS1 end point in both planes. The maximum of the beta function can be limited to below 100 m in the horizontal and below 200 m in the vertical plane.

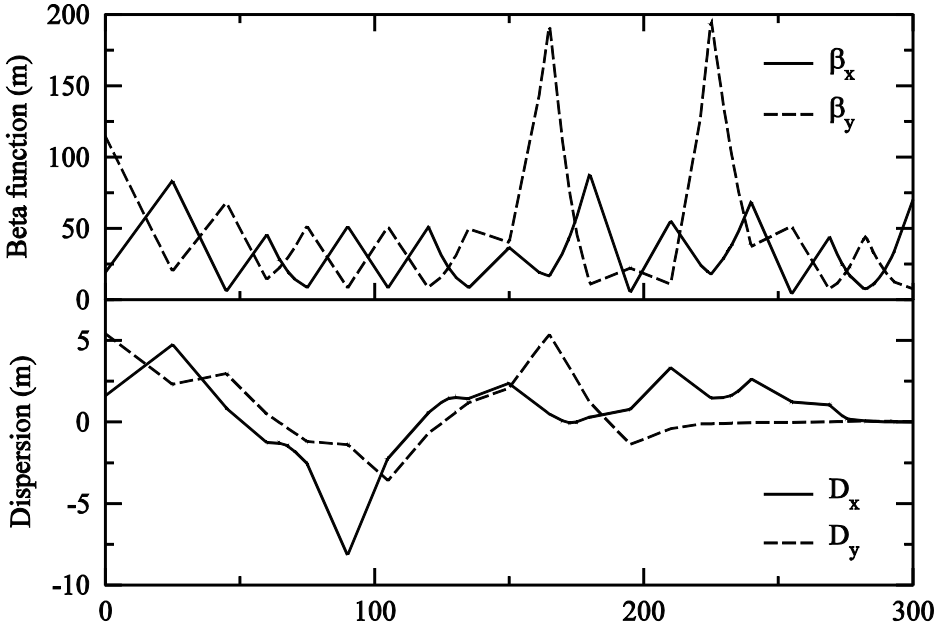

Figure 10 Simulated beta and dispersion functions along the new part of the TT10 transfer line for a proton beam using MAD-X

4.3 Aperture studies

Aperture calculations which have been carried out for the new part of TT10 using Eqn. (2) yield large beam envelope values for the 1.3 GeV proton beam case. These studies are based on normalized horizontal and vertical emittances $\varepsilon_{xn} = \varepsilon_{yn} = 3$ μm and a momentum spread of $\Delta p/p = 0.001$. Detailed beam envelope calculations for different beam sizes and maximum trajectory excursions of 5 and 10 mm are presented in Figs. 11 and 12, respectively. To be noted, the maximum trajectory excursion in the existing part of the beam line is rather 10 mm.

It was planned to use the same magnet types as in the present TT10 transfer line whose aperture limits are also plotted in Figs. 11 and 12. These figures show that at the location of the quadrupoles, beam sizes of 4 and 3.5 σ are feasible if the maximum trajectory excursion is limited to 5 and 10 mm, respectively. However, the aperture of the foreseen bending magnet types MBIH and MBIV is not sufficient even for a 3 σ beam size. For the LHC proton beam for PS2 commissioning this is less of an issue, as a small 1 μm emittance 'pilot' type beam can be used, however for the ion beam the losses may be too high. Further studies will take this into account.

In order to reduce the beam loss it is proposed to equip the existing and the new part of TT10 with a sufficient number of beam position monitors so that a maximum trajectory excursion of 5 mm can be ensured. A list with the draft magnet specifications is shown in Tab. 11, including their original aperture and the aperture needed for a 6 σ beam size.

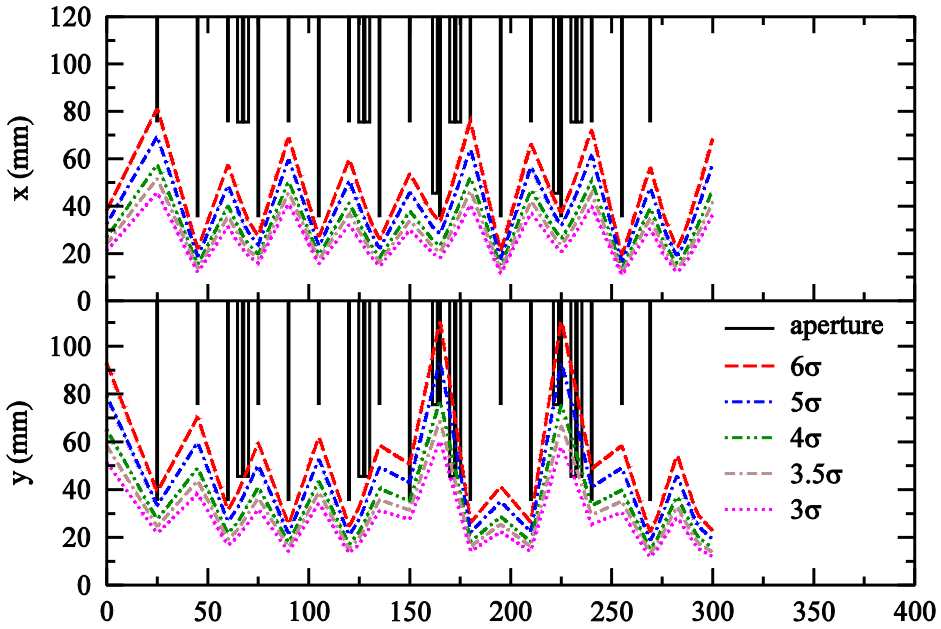

Figure 11 Beam envelope calculations of the new part of the TT10 transfer line for a 1.3 GeV proton beam with a maximum trajectory excursion of 5 mm and different beam sizes

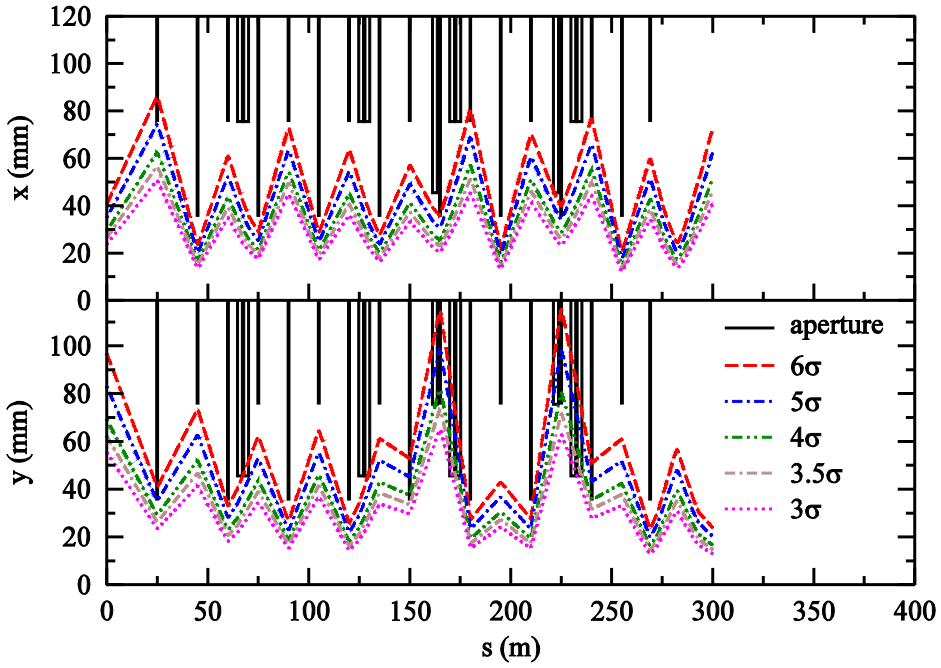

Figure 12 Beam envelope calculations of the new part of the TT10 transfer line for a 1.3 GeV proton beam with a maximum trajectory excursion of 10 mm and different beam sizes

Table 11: Draft specifications of the magnets for the new part of the TT10 transfer line.

Magnet type	Max. grad. or field	Length	Max. K or α	Number	Half aperture H, V [m]		
					Original	co=5 mm	co=10 mm
QIF	7 T/m	0.5 m	0.4 m^{-2}	17	0.076/0.036	0.08/0.055	0.085/0.06
QID					0.036/0.076	0.04/0.11	0.045/0.12
MBIV	0.25 T	2.5 m	0.04 rad	2	0.046/0.076	0.045/0.11	0.05/0.115
MBIH	0.6 T	2.5 m	0.09 rad	8	0.076/0.046	0.065/0.095	0.07/0.1

5. TT11 transfer line

The TT11 transfer line will link the PS2 to the SPS. Its upstream part will be in common with the TTEA beam line, linking the PS2 to a new PS2 fixed target experimental area. Both proton and ion beams will be transported through TT11. The latter requires a stripping foil in the beam line to strip the Pb^{54+} ions from LEIR to Pb^{82+} before their injection into the SPS. Furthermore, the option to exchange the horizontal and vertical emittance for fixed target proton beams for the SPS has not been excluded [11] and therefore a dedicated emittance exchange section in the beam line has been investigated.

5.1 Beam line geometry

The layout of TT11 (Fig. 13) is based on a FODO lattice with 21 m cell length and 90° phase advance per cell [12]. The Twiss functions are fully matched at both ends to the PS2 and the SPS using either regular cell quadrupoles or a dedicated matching section (Tab. 12). The end section of the present TT10 and the SPS injection region geometry are kept and reused for the injection layout of TT11 into SPS.

Two horizontal achromats are used. Due to the fact that TT11 is located in the same plane as PS2 and SPS no vertical dipole magnets are needed. Between the two achromats a 2.5-cell dispersion free section with three skew quadrupoles has been designed, acting as a "perfect" emittance exchange section [13]. A low beta section housing the stripping foil for heavy ion beams is installed in the matching section.

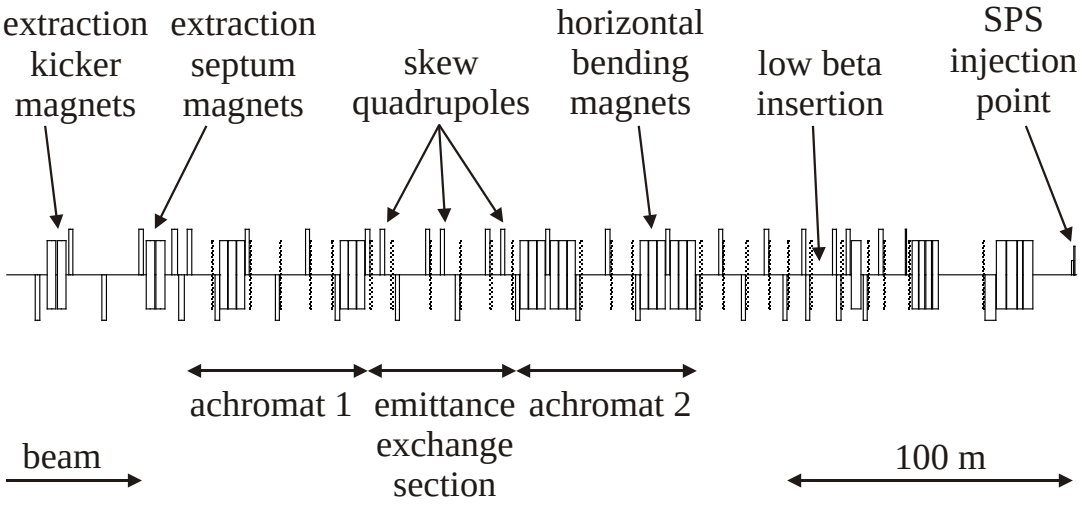

Figure 13 Beam line layout of the TT11 transfer line

Table 12: Twiss parameters at the start and the end point of the TT11 transfer line (in beam direction).

Point	Plane	β [m]	α	D [m]	D'
LSS1 start	X	33.925	2.073	0	0
	Y	12.495	-0.810	0	0
SPS inj. point (BPH.12008.E)	X	101.731	-2.292	0.01757	0.009511
	Y	21.328	0.561	0	0

Table 13: CCS coordinates of the start and the end points of TT11 (in beam direction). The starting point of the extraction kicker PS2.EXTK2B is listed and used as a reference point for PS2 survey calculation.

Point	X [m]	Y [m]	Z [m]	Bearing [rad]	Slope [rad]
PS2 LSS1 start	1237.01686	2468.32362	2402.16289	-0.75042	-0.000207
PS2.EXTK2B start	1227.31886	2478.72486	2402.15994	-0.75042	-0.000207
SPS inj. point (BPH.12008.E)	981.65915	2737.00508	2402.08645	-0.95539	-0.000179

5.2 Optics simulations

Detailed optics studies have been performed, for the cases with skew quadrupoles powered and not. For the latter case, simulations have been carried out with MAD-X and the resulting beta and dispersion functions are shown in Fig. 14. The maximum beta function is about 200 m and the dispersion between the two achromats is zero as required by the emittance exchange section [13].

In case of coupled motions MAD-X produces incorrect results [14] and the PTC_TWISS module [15] of MAD-X must be used. The resulting Ripken optics parameters β_{11}, β_{22}, β_{12} and β_{21}, calculated for the skew quadrupoles switched on, are shown in Fig. 15 together with the dispersion functions. For this simulation the quadrupole strengths of the uncoupled case were taken as starting values. In a first step the emittance exchange section was matched to the rest of the line and in a second step the beam line was rematched to the SPS. A calculation of the normalized emittance growth due to dispersion mismatch at the SPS injection point, using Eqn. (3), yielded zero in both planes,

$$\Delta\varepsilon_{norm} = \frac{\beta_r\gamma_r}{2}\frac{\Delta D^2 + \left(\beta\Delta D' + \alpha\Delta D\right)^2}{\beta}\left(\frac{\Delta p}{p}\right)^2 \qquad (3)$$

where β_r and γ_r are the relativistic factors, α, β, D, D' the optics functions and $\Delta p/p$ the momentum spread. This result shows that the emittance exchange section works as intended. The maximum beta function is of the same order as for the uncoupled case.

The simulations resulted in large strengths of the low-beta insertion quadrupoles and the nearby regular matching quadrupoles. Therefore, further optimisations of the low-beta insertion are necessary if this layout is chosen for the final beam line.

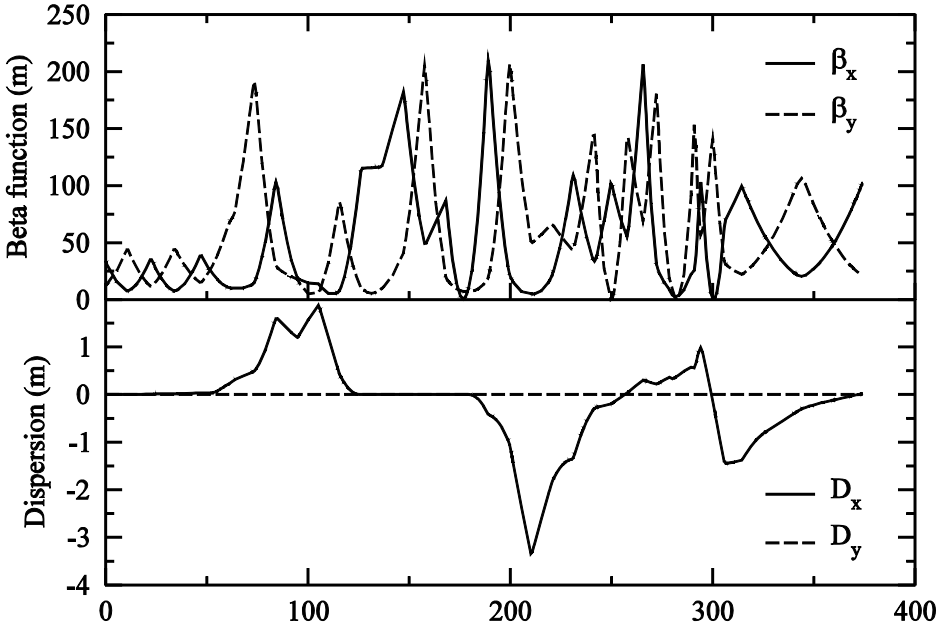

Figure 14 Simulated beta and dispersion functions along the TT11 transfer line for a proton beam with the emittance exchange section switched off, using MAD-X

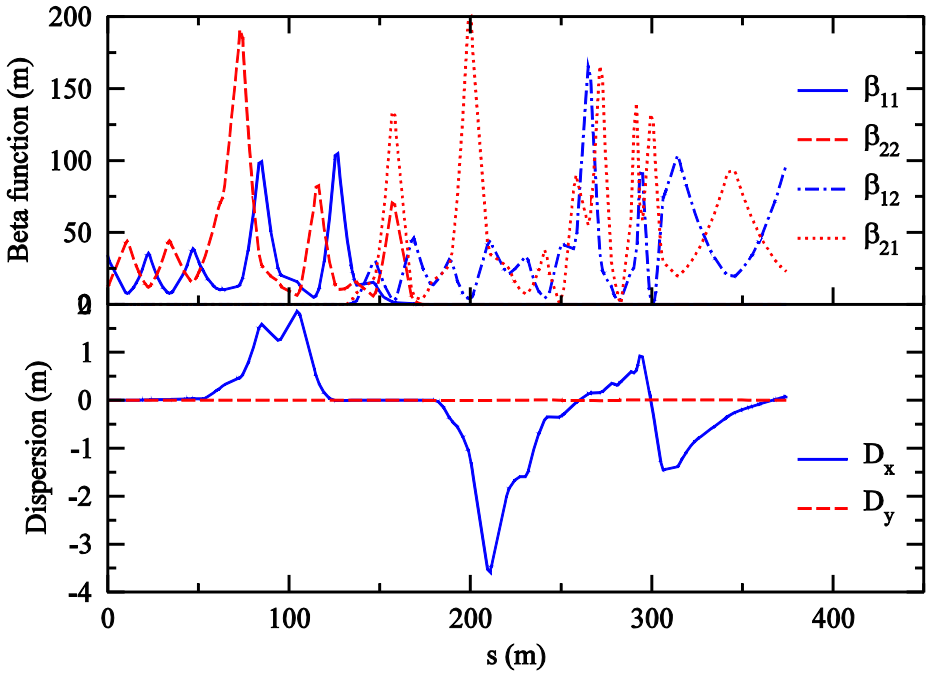

Figure 15 Simulated beta and dispersion functions along the TT11 transfer line for a proton beam with the emittance exchange section switched on, using MAD-X with the PTC_TWISS module

5.3 Aperture calculations

Aperture calculations have been performed for the TT11 beam line optics with the emittance exchange section switched off, Eqn. (2). Due to the similar maximum beta function values, the result can be transferred to the coupled case. The calculations have been carried out for a 20 GeV proton beam with normalized horizontal and vertical emittances of ε_{xn} = 9 µm and ε_{yn} = 7 µm [11], respectively. The assumed rms beam size was 6 σ, the maximum trajectory excursions 5 mm and the momentum spread $\Delta p/p$ = 0.001. This results in a maximum needed half aperture of 65 mm in the horizontal plane and 55 mm in the vertical plane (Fig. 16). The aperture requirements of the magnets are summarized in Tab. 14, together with the draft magnet specifications.

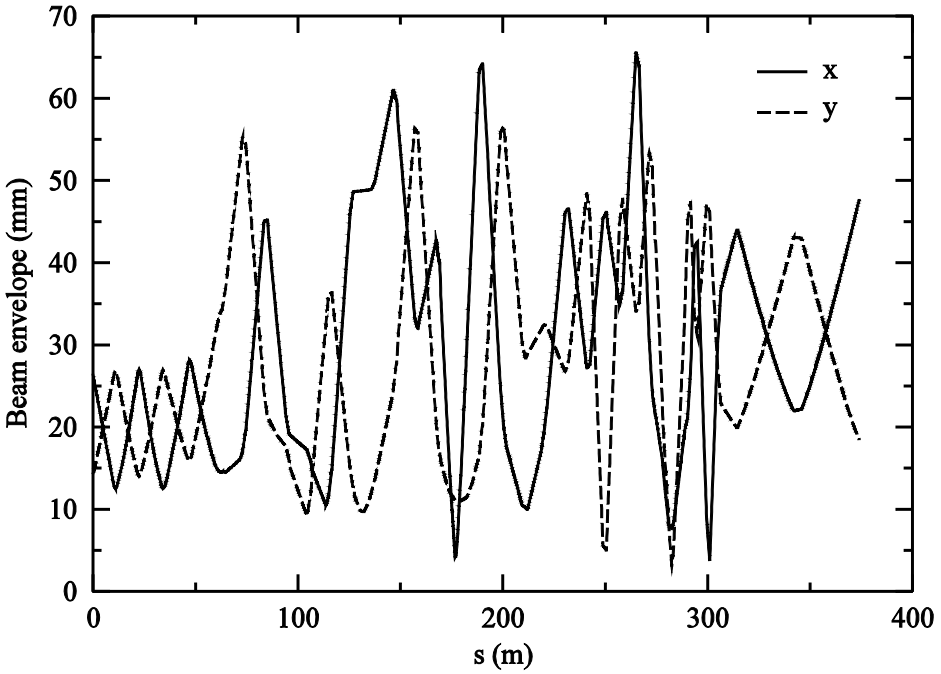

Figure 16: Plot of the calculated beam envelopes along TT11 in the horizontal and vertical plane for a 20 GeV proton beam with the emittance exchange section switched off.

Table 14: Draft TT11 magnet specifications. One main quadrupole with an enlarged horizontal half aperture of 0.09 m is needed for the crossing point with TTL1.

Magnet type	**Max. gradient or max. field**	**Length**	**Max. K or max. α**	**Number**	**Half aperture H/V**
MQ main	24 T/m, 54 T/m	1.477 m	0.14 m^{-2}, 0.32 m^{-2}	27	0.07 m / 0.06 m
MQ low beta	32 T/m	1.477 m	0.19 m^{-2}	2	0.07 m / 0.06 m
MQ skew	10 T/m	1.477 m	0.06 m^{-2}	3	0.07 m / 0.06 m
MB	1.7 T	2.789 m	0.028 rad	18	0.07 m / 0.06 m

5.4 Trajectory correction

It is not possible to implement a regular combined 1-in-1 / 2-in-3 scheme in TT11, as done in TTL1, due to the limited space in the FODO half cells equipped with bending magnets. The free space between the magnets is not sufficient to house any equipment. In these half cells, the monitors and the correctors have been placed in front of the first quadrupole, instead of behind it, and behind the last quadrupoles. In addition, in FODO cells fully equipped with bending magnets, the monitors and correctors at the central quadrupole have been dropped. In the remaining cells, only a few correctors could be dropped to approximate a combined 1-in-1 / 2-in-3 scheme.

For this scheme the same errors as for TTL1 (Tab. 8) have been assumed, with the exception of the injection errors. Figure 17 shows a plot of 100 simulated uncorrected and corrected trajectories for the described scheme. The calculated corrector strength is below 0.06 T and the corrected trajectory excursions are in most cases less than 1.5 mm, except at the locations where space is missing for a corrector and monitor – inside the fully equipped FODO cells and at the TT10 bending magnet MAL.102928. This affects only the horizontal trajectories and might improve if the main bending magnets at these locations are additionally used for correction. Furthermore, there are a few cases where the trajectory could not be corrected at the end of the beam line, and this was always due to a failure of the last monitor. The influence of the trajectory correction on the dispersion is shown in Fig. 18.

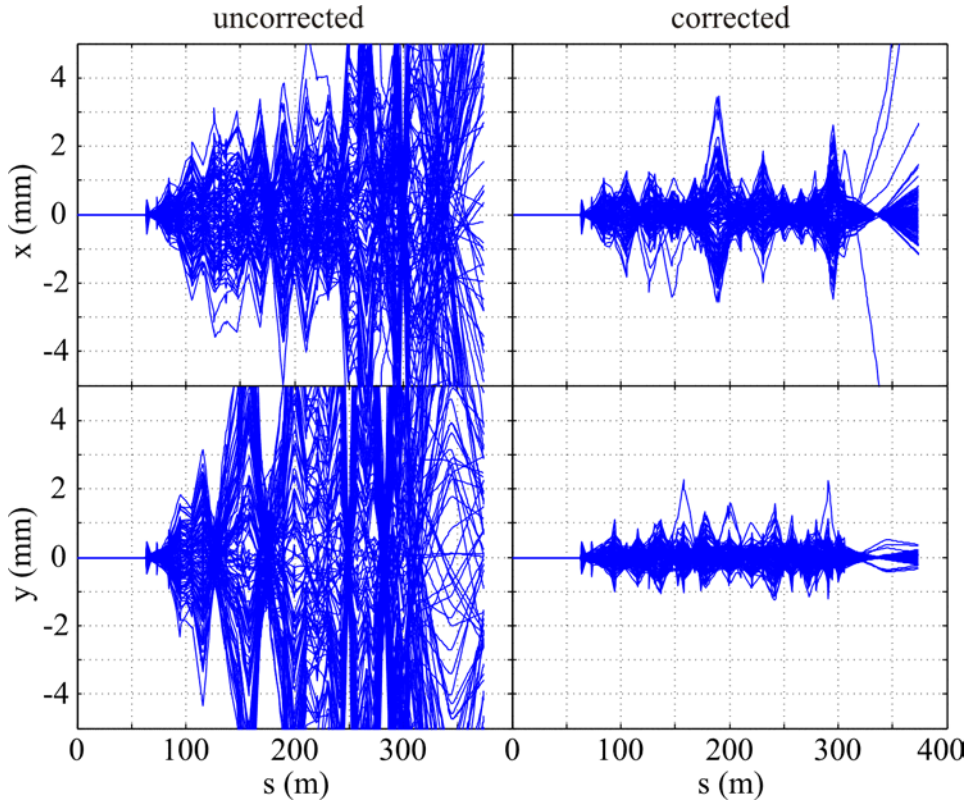

Figure 17 Plot of 100 uncorrected and corrected trajectories for TT11 (emittance exchange section switched off)

The trajectory correction simulations for TTL1 have been carried out with MAD-X using the MICADO algorithm. Due to the fact that the error correction module of MAD-X cannot deal with Ripken style Twiss parameter tables, only the uncoupled case with the emittance exchange section switched off could be studied.

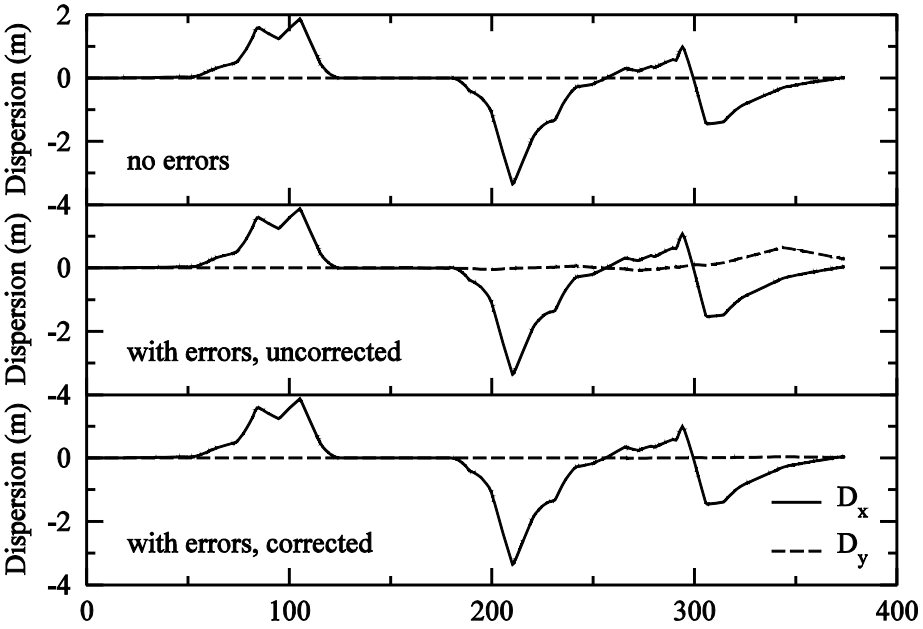

Figure 18 Influence on the dispersion resulting from assigned errors. No errors (top), with errors (center), corrected trajectories (bottom)

6. TTEA beam line

The TTEA beam line will branch off TT11 and serve a new PS2 fixed target experimental area with 20 to 50 GeV proton beams extracted from PS2 by slow extraction. In addition this beam line will also transport fast extracted proton and heavy ion beams to an external beam dump. So far, only very preliminary studies of this beam line have been carried out to investigate its integration into the injection/extraction region.

6.1 Beam line geometry

The TTEA transfer line splits off TT11 behind the first half cell of the emittance exchange section of TT11, which must be switched off during TTEA operation. The CCS coordinates of the starting point of TTEA are listed in Tab. 17. The TTEA is based on a FODO lattice with 90° phase advance per cell like in TT11. In order to avoid physical interference between the TT11 and TTEA quadrupoles at the branching point, a slightly larger cell length (26.25 m) than in TT11 was chosen. For the branching, MBS like switching magnets are used, installed in an empty half cell of the TT11 emittance exchange section. The switching magnets form an achromat together with three further half cells equipped with regular bending magnets and an empty cell in between it (Fig. 19). The magnet types are the same as the ones foreseen for the TT11 transfer line. Their draft specifications are summarized in Tab. 18.

Table 17: CCS coordinates of the starting point of TTEA (in beam direction) which is the end of quadrupole MQF.5 in TT11.

Point	X [m]	Y [m]	Z [m]	Bearing [rad]	Slope [rad]
PS2 LSS1 start	1149.91737	2574.247045	2402.133475	-0.56036	-0.000226

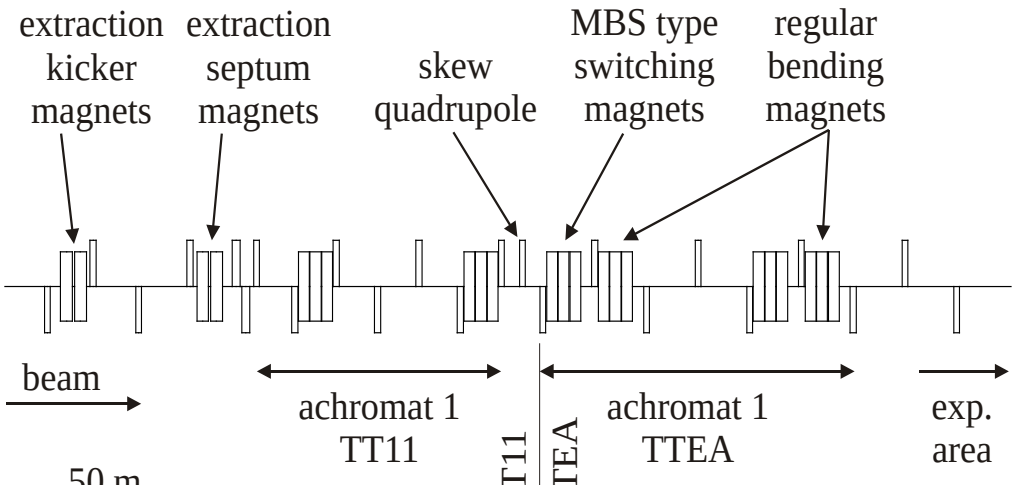

Figure 19 Layout of the upstream part of the TTEA beam line

Table 18: Draft TTEA magnet specifications.

Magnet type	**Max. gradient or max. field**	**Length**	**Max. K or max. α**	**Number**	**Half aperture H/V**
MQ main	16 T/m,	1.477 m	0.09 m^{-2}	8 + X	0.04 m / 0.04 m
MB	1.7 T	2.789 m	0.028 rad	9 + X	0.04 m / 0.04 m
MBS	1.7 T	2.789 m	0.028 rad	3	0.04 m / 0.04 m

6.2 Optics simulations

For this layout detailed optics simulations have been carried out with MAD-X for fast and slow extracted beams. In the first case the start of the LSS1 in the PS2 was used as starting point for the simulations, using the same Twiss parameters at the starting point as for TT11 (Tab. 12). For the slow extracted beam, however, the electro-static septum was used as starting point. In this case, the horizontal Twiss parameters (Tab. 19) were obtained by fitting an ellipse to a phase space area computed in Ref. [16]. This procedure yielded also the horizontal normalized emittance $\varepsilon_{xn,slow}$ = 0.45 µm of the slow extracted beam. The vertical Twiss parameters and emittance are the same as for the fast extracted beam.

Table 19: Twiss parameters for the slow extracted beam at the start of the electro-static septum of the TTEA transfer line (in beam direction).

Point	**Plane**	**β [m]**	**α**	**D [m]**	**D'**
Start of electro-static septum	X	97.935	3.539	0.011	0.0003
	Y	14.302	-0.946	0	0

The results for the fast and the slow extracted beam are shown in Figs. 20 and 21, respectively. The betatron oscillation for both beams is regular with zero dispersion after the achromat. This allows an easy extension of the beam line to a possible PS2 fixed target experimental area. The horizontal betatron function of the slow extracted beam is much larger than of the fast extracted beam. However, due to the smaller horizontal emittance this is not an issue.

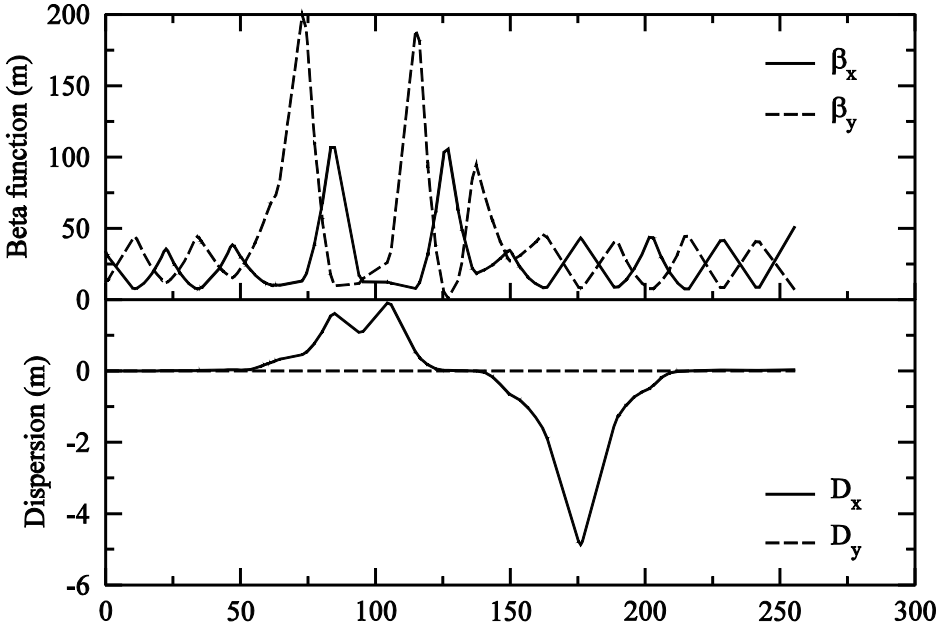

Figure 20 Simulated beta and dispersion functions along the TTEA transfer line (including the upstream part of TT11) for a fast extracted proton beam using MAD-X

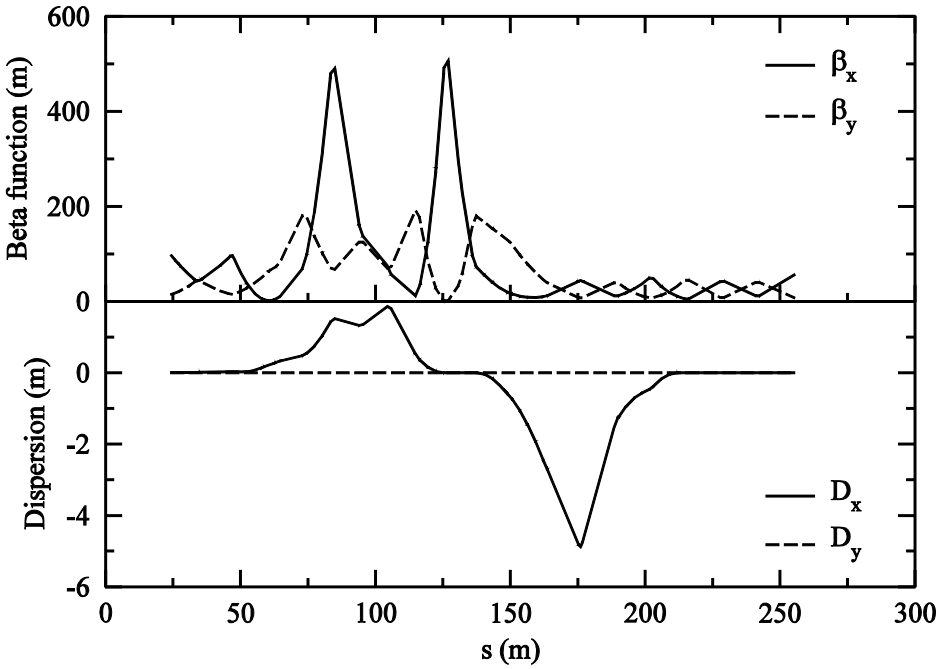

Figure 21 Simulated beta and dispersion functions along the TTEA transfer line (including the upstream part of TT11, starting at the electro-static septum) for a slow extracted proton beam using MAD-X

6.3 Aperture calculations

Beam envelope calculations have been performed for fast and slow extracted 20 GeV proton beams and are shown in Figs. 22 and 23, respectively. For the fast extracted beam the same parameters were used as for TT11 (section 5.3), whereas the modified horizontal normalized emittance $\varepsilon_{xn,slow}$ = 0.45 µm was used for the slow extracted beam. The results show that the requirements on the aperture are much more relaxed than in TT11. A half aperture of 40 mm is sufficient in both planes for both beams.

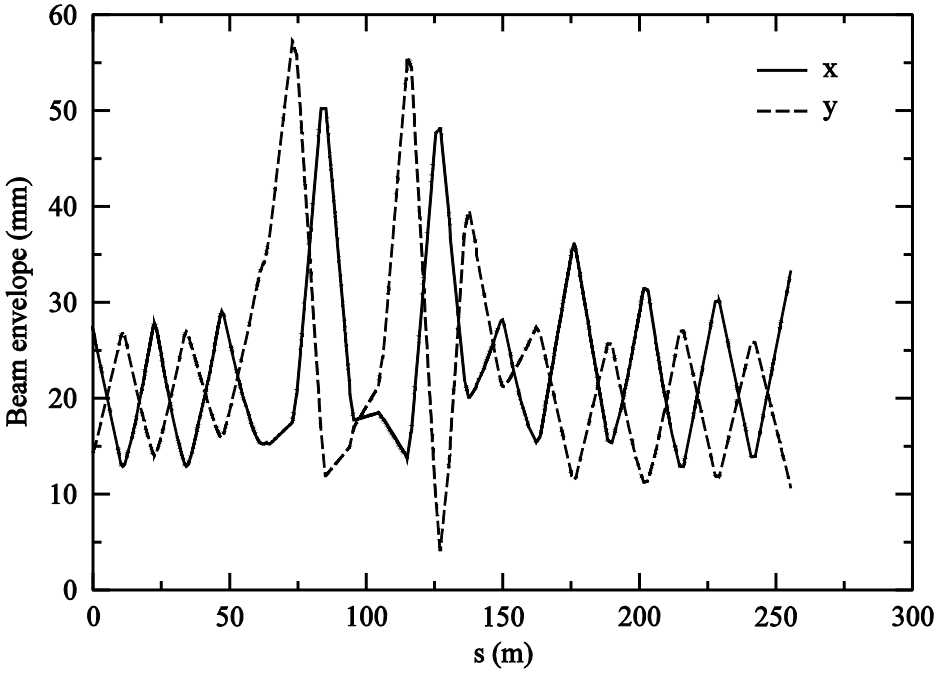

Figure 22 Plot of the calculated beam envelopes along TTEA (including the upstream part of TT11) in the horizontal and vertical plane for a fast extracted 20 GeV proton beam

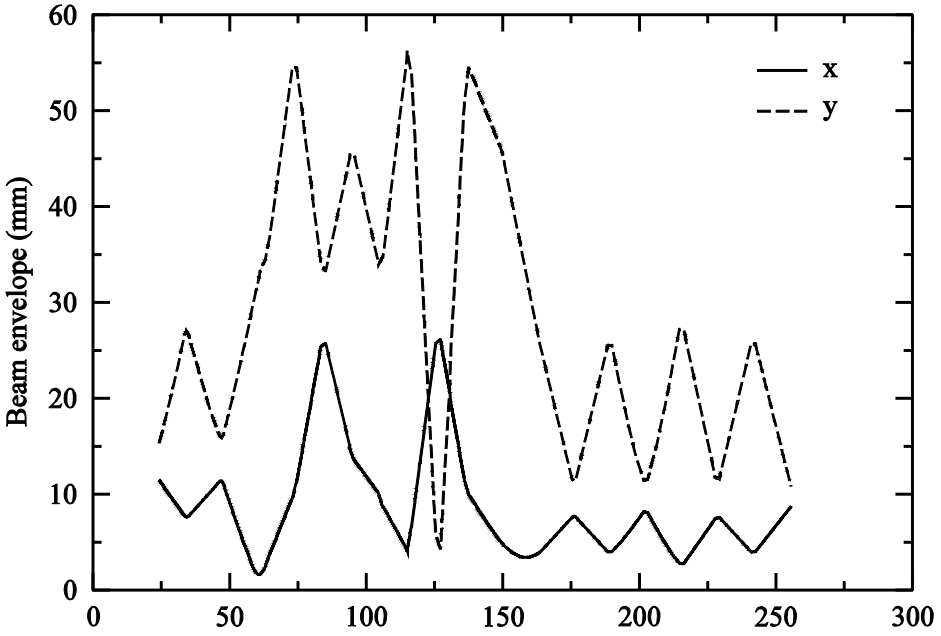

Figure 23 Plot of the calculated beam envelopes along TTEA (including the upstream part of TT11, starting at the electro-static septum) in the horizontal and vertical plane for a slow extracted 20 GeV proton beam

7. TD1 beam line

The TD1 beam line starts at the stripping foil and transports the waste beam to a nearby beam dump. The waste beam is generated by the non-perfect stripping process during charge exchange injection and consists of unstripped H^- and partially stripped H^0. In order to form a uniformly charged waste beam, a second thick stripping foil with high efficiency is placed behind the third chicane magnet [5]. The TD1 beam line consists only of one MBIH magnet which deflects the beam into the beam dump which is located approximately 25 m further downstream. Beam envelope calculations showed that no focussing is necessary over this short distance (Fig. 24).

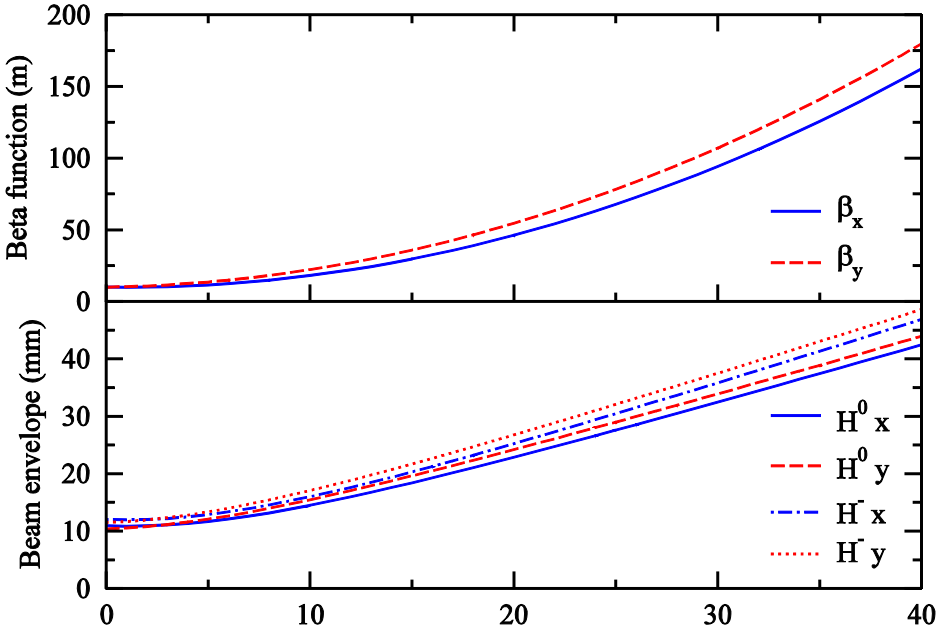

Figure 24 Plot of the beta functions and the beam envelopes of unstripped H^- and partially stripped H^0 beams. Equation (2) was used for the beam envelope calculation. A momentum spread of 0.002 and normalized emittances of 1 and 1.25 μm were assumed for H^0 and H^- beams, respectively. The other parameters are the same as for TTL1

8. Injection and extraction region geometry

Due to the chosen injection/extraction concept with the extraction point upstream of the two injection points, the layout of the injection/extraction region is challenging. The beam lines cross each other at several points in the same plane:

- TT11 and TTL1;
- TT11 and TT10;
- TT11 and TD1;
- TT10 and TD1.

In this chapter studies of the injection/extraction region geometry are presented. For that purpose, the widths listed in Tab. 20 have been assumed for the beam line elements. These values are rough estimates and will be refined when more precise magnet dimensions are available. The geometry of the beam lines have been plotted with MATLAB [17] based on these assumptions and on survey data generated with MAD-X. For more precise investigations, detailed magnet design studies have to be carried out.

Table 20: Assumed widths of the beam line elements used for the geometry plots.

Element	Width [m]
H^- beam dump	2.4
Beam position monitors	0.3
Regular PS2 quadrupoles	1.2
Enlarged PS2 quadrupoles	1.44
All other elements	0.5

An overview on the injection/extraction region and a more detailed drawing of the crossing region of TT11, TT10 and TD1 are shown in Figs. 25 and 26, respectively. Although this crossing region layout imposes some restrictions on the serviceability of some parts of the beam lines, there are no interferences between the elements of the different beam lines.

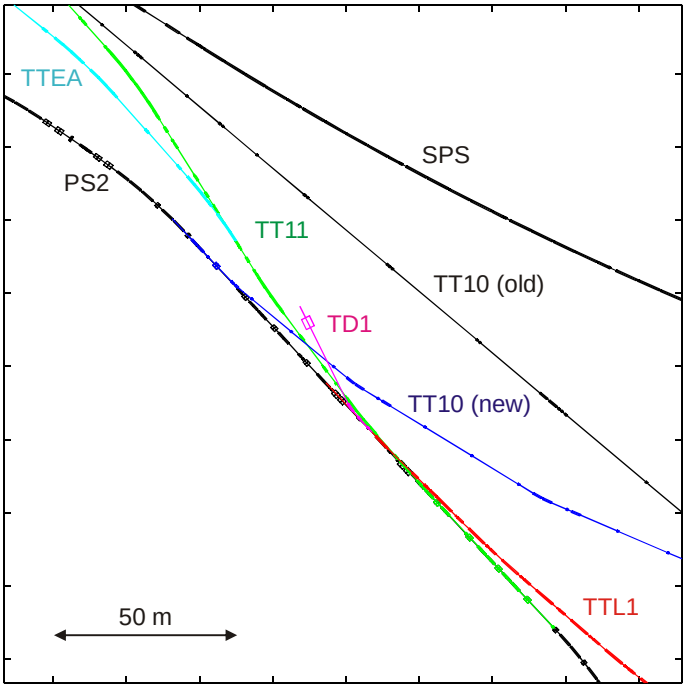

Figure 25 Overview on the injection/extraction region

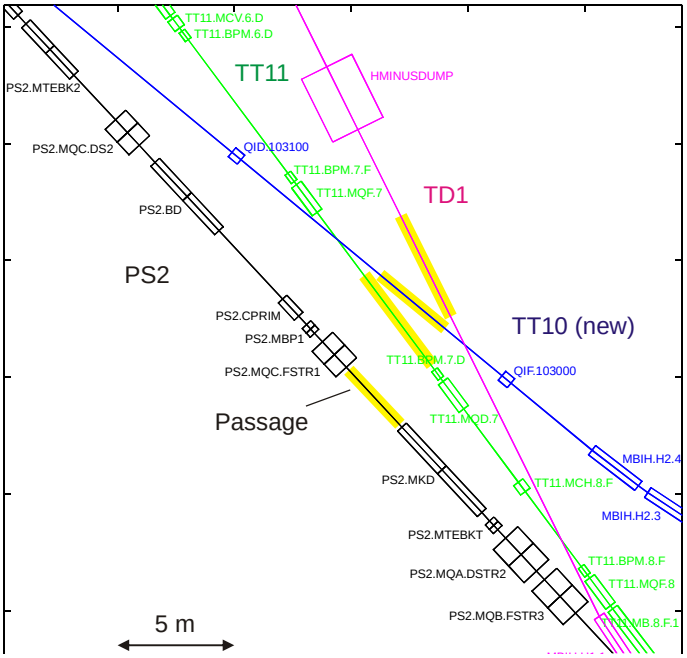

Figure 26 Overview on the crossing region of TT11, TT10 and TD1. The yellow bars indicate possible locations for removable beam line sections to allow the passage of equipment

In contrast, the situation at the TT11/TTL1 crossing is much tighter due to the small injection and extraction angles which are caused by the Lorentz stripping limit and the finite strength of the extraction septa. An overview of this region is shown in Fig. 27.

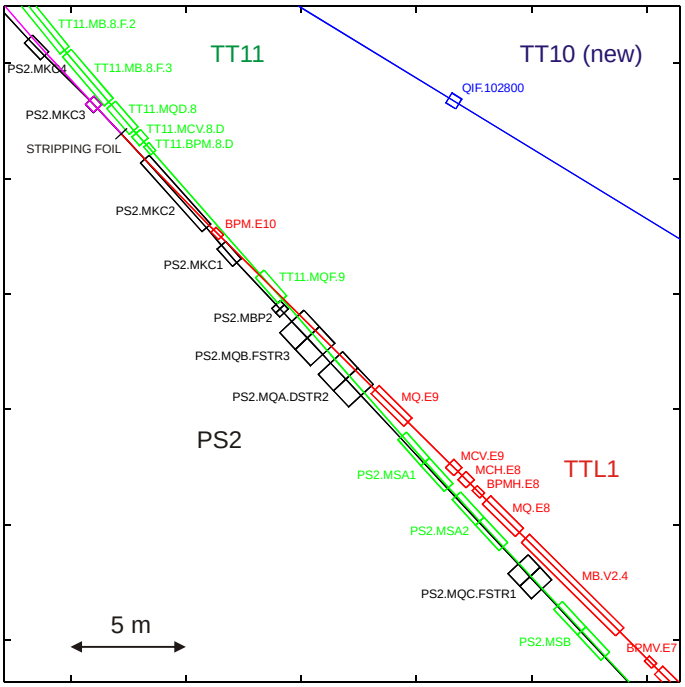

Figure 27 Overview on the crossing region of TT11 and TTL1

Near the H^- injection chicane, the PS2, TTL1 and TT11 beam lines are close together. Therefore, C-shaped dipole magnets must be used for the PS2 injection chicane magnets MKC1, MKC2, MKC3 and MKC4 and most likely also for the first TT11 main bending magnets (Fig. 28).

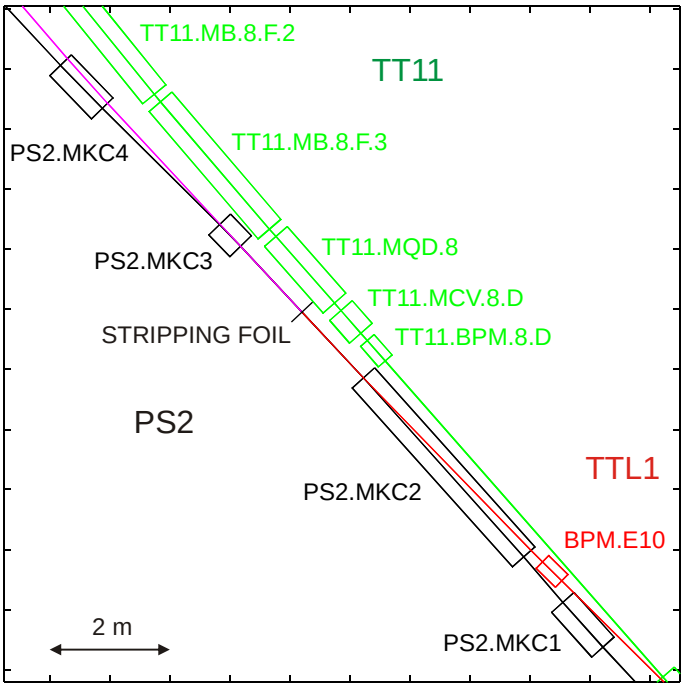

Figure 28 Layout of the H^- injection chicane and the nearby TT11 extraction beam line

TTL1 and TT11 cross each other in the center of the TT11 quadrupole MQF.9 which requires therefore an enlarged horizontal half aperture of 90 mm. Furthermore, both beam lines have to cross the adjacent PS2 quadrupoles MQB.FSTR3 and MQA.DSTR2 at distances from their central axis varying from 189 to 615 mm (Fig. 29). This requires special quadrupoles with coil windows for the passage of the TT11 beam line. Feasibility studies of this special magnet design have still to be carried out.

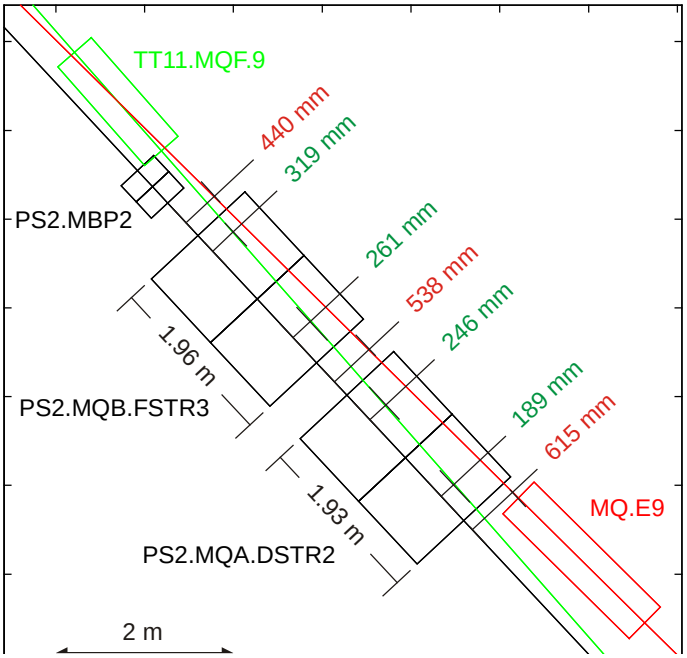

Figure 29 TT11/TTL1 crossing and the adjacent special quadrupoles

At the branching point of TTEA and TT11 the beam lines are also very close together (Fig. 30), which must be taken into account for the magnet design of the TT11 quadrupoles. The deflection angle of the MBS switching magnets cannot be further increased due to their powering limit of 1.7 T.

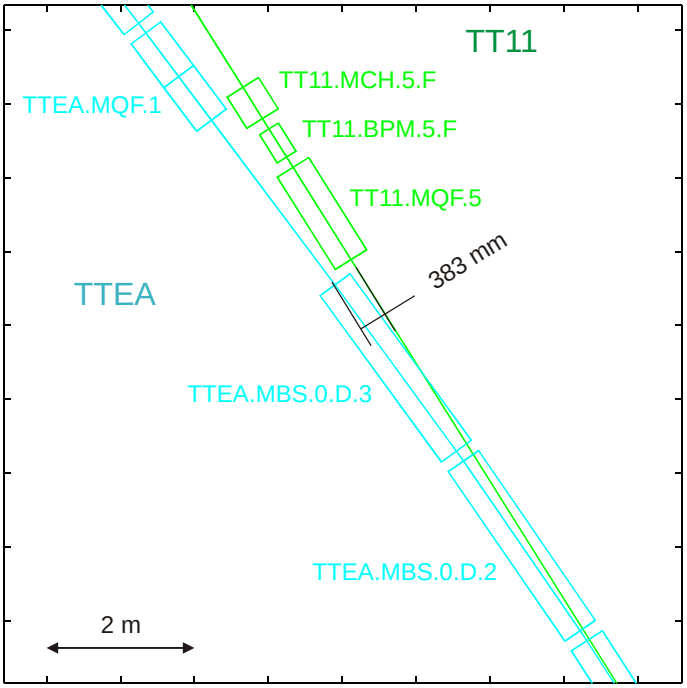

Figure 30 Branching point of TTEA and TT11

7. Conclusion

The feasibility of the various beam lines needed for the PS2 injection and extraction has been investigated based on the present PS2 injection/extraction concept, with the extraction point located upstream of the injection points. The presented beam line designs fulfil all geometrical and matching constraints as well as the Lorentz stripping limit for TTL1. However, the intersections of the beam lines in the injection/extraction region are complicated and impose severe constraints on the magnet design which must be checked in detail. The assumption of 0.5 m wide quadrupole and dipole magnets is possibly too optimistic. An optimisation of the injection/extraction region to avoid these complications and the associated constraints is therefore under study.

Further work has also to be carried out on the ion optics of TT11, including the low-beta section for stripping Pb^{54+} to Pb^{82+} ions. In addition to present optics simulations with MAD-X at zero beam current, simulations which include multi-particles and space-charge effects are planned and have already started for TTL1 [18].

8. Acknowledgements

The authors would like to thank many CERN colleagues for their contributions and fruitful discussions, in particular W. Bartmann, M. Benedikt, M. Eshraqi, F. Gerigk, M. Gyr, W. Herr, M. Jones, A. Kosmicki, A. M. Lombardi, L. A. Lopez-Hernandez, D. Missiaen, J. A. Osborne, M. Poehler, G. de Rijk, F. Schmidt and J. Uythoven. In addition, the significant initial work of A. Koschik is gratefully acknowledged.

References

[1] R. Garoby, “Plans for Upgrading the CERN Proton Accelerator Complex”, Proc. International Europhysics Conference on High Energy Physics 2007, Manchester, J. Phys.: Conf. Ser. 110 (2008) 112003.

[2] L. Arnaudon et al., “Linac4 Technical Design Report”, CERN-AB-2006-084 (2006).

[3] O. Brunner et al., “Plans for a Superconducting H^- LINAC (SPL) at CERN”, CERN-AB-2008-066 BI (2008).

[4] M. Benedikt, “Design Optimization of PS2”, Proc. PAC’09, Vancouver, in press.

[5] W. Bartmann, M. Benedikt, B. Goddard, “A Triplet Insertion Concept for the PS2 H^- Injection”, Proc. ICFA Advanced Beam Dynamics Workshop on High-Intensity, High-Brightness Hadron Beams 2008, Nashville, in press.

[6] B. Goddard, W. Bartmann, D. E. Johnson, V. V. Danilov, “Laser Stripping for the PS2 Charge-Exchange Injection System”, Proc. PAC’09, Vancouver, in press.

[7] A. J. Jason, D. W. Hudgings, O. B. van Dyck, “Neutralization of H^- beams by magnetic stripping”, IEEE Trans. Nucl. Sci. NS-28 (1981) p. 2704.

[8] J. Gervaise, M. Mayoud, E. Menant, “Système tridimensionnel de coordonnées utilisé au CERN”, CERN 76-03 (1976).

[9] M. Jones, private communication.

[10] www.cern.ch/mad.

[11] G. Arduini et al, “Considerations on the Transverse Emittance of the Fixed-Target Beam in the SPS in the PS2 Era”, CERN-BE-Note-2009-025 (2009).

[12] W. Bartmann, M. Benedikt, B. Goddard, T. Kramer, A. Koschik, “PS2 Injection, Extraction and Beam Transfer Concepts”, Proc. PAC’07, Albuquerque, 2007, p. 1598.

[13] L. R. Evans, “A Phase Plane Exchange Section for the SPS Antiproton Injection Beam-Line”, CERN-SPS-DI-MST 80-2 (1980).

[14] O. Berrig, “TT10 optics with emittance exchange. MAD8 vs. PTC”, LIS Section Meeting, 19.02.2007.

[15] F. Schmidt, “MAD-X PTC Integration”, Proc. PAC’05, Knoxville, 2005, p. 1272.

[16] M. Gyr, W. Bartmann, M. Benedikt, B. Goddard, M. Meddahi, A. Koschik, D. Mayani Parás, “Resonant Third-Integer Extraction from the PS2”, Proc. PAC’09, Vancouver, in press.

[17] www.mathworks.com/products/matlab.

[18] C. Hessler, M. Eshraqi, B. Goddard, A. M. Lombardi, M. Meddahi, “The 4 GeV H^- Beam Transfer Line from the SPL to the PS2”, Proc. PAC’09, Vancouver, in press.